Dynamical Analysis of 1:1 Resonances near Asteroids: Application to Vesta

S. Broschart[1] J.M. Mondelo[2] B.F. Villac[3]

[1]Jet Propulsion Laboratory, California Institute of Technology

[2]Universitat Autònoma de Barcelona

[3]University of California at Irvine

Seminari de sistemes dinàmics UB–UPC,
12 de gener de 2011

Motivation & goals

- **Motivation:**
  - DAWN rendezvous with Vesta in July, 2011.
    Propulsion: Ion engine + att. thrusters.
    Orbits:
    - Survey @ 2700 km,
    - HAMO @ 950 km,
    - LAMO @ 460 km, below 1:1 res.

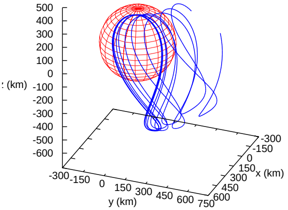

  - Leverage knowledge of unstb. equilibria and p.o. in simplified models (e.g. Scheeres 1994) to a full model using dynamical systems techniques.
  - Resonant orbit dynamics are generally chaotic in the 1:1 resonance region.

- **Goal:**
  Use resonant dynamics to design and characterize ballistic transfers across the 1:1 resonance.

Outline

1. Model setting
2. Resonant dynamics
3. Ballistic resonance crossing
4. Polar families of p.o.
5. Conclusions

Outline

1. Model setting
2. Resonant dynamics
3. Ballistic resonance crossing
4. Polar families of p.o.
5. Conclusions

Equations of motion (1)

- Consider an irregular body C.
- Split it in N pieces with masses $m_1, \ldots, m_N$ and inertial positions $\boldsymbol{R}_1, \ldots, \boldsymbol{R}_N$.
- Denote by $\boldsymbol{R}$ the inertial position of the spacecraft, by m its mass.
- Denote by $\rho(m_i)$ the density of the piece of mass m_i, by $\mathrm{vol}(m_i)$ its volume.
- From the Newtonian attraction of the N pieces of the body:

$$
\begin{aligned}
m\ddot{\boldsymbol{R}} &= -\sum_{i=1}^{N} \frac{Gmm_i}{\|\boldsymbol{R}-\boldsymbol{R}_i\|^3}(\boldsymbol{R}-\boldsymbol{R}_i) \\
\ddot{\boldsymbol{R}} &= -\sum_{i=1}^{N} \frac{G\rho(m_i)\,\mathrm{vol}(m_i)}{\|\boldsymbol{R}-\boldsymbol{R}_i\|^3}(\boldsymbol{R}-\boldsymbol{R}_i) \\
&\downarrow \quad N\to\infty \\
\ddot{\boldsymbol{R}} &= -\int_C \frac{G\rho(\boldsymbol{Q})}{\|\boldsymbol{R}-\boldsymbol{Q}\|^3}(\boldsymbol{R}-\boldsymbol{Q})d\boldsymbol{Q}
\end{aligned}
$$

- This is for a **non–rotating** body.

Equations of motion (2)

- If the body rotates uniformly, the previous argument applies for each time instant.
- Denote by C_0 the body at time t_0, ρ_0 the density defined over C_0.
- Then at time t the body is $C(t) = M(\omega(t-t_0))C_0$, being $M(\theta)$ the rotation of angle θ around its axis, and ω its angular frequency.
- Consider rotating coordinates $\boldsymbol{r}$ defined by

$$\begin{aligned}
\boldsymbol{R} &= M\boldsymbol{r}, \\
\dot{\boldsymbol{R}} &= M(\dot{\boldsymbol{r}} + \boldsymbol{\omega} \times \boldsymbol{r}), \\
\ddot{\boldsymbol{R}} &= M(\ddot{\boldsymbol{r}} + \underbrace{2\boldsymbol{\omega} \times \dot{\boldsymbol{r}}}_{\text{Coriolis}} + \underbrace{\dot{\boldsymbol{\omega}} \times \boldsymbol{r}}_{\text{Euler}=0} + \underbrace{\boldsymbol{\omega} \times (\boldsymbol{\omega} \times \boldsymbol{r})}_{\text{centrifugal}}),
\end{aligned}$$

where

$$M^\top \dot{M} = \begin{pmatrix} 0 & -\omega_3 & \omega_2 \\ \omega_3 & 0 & -\omega_1 \\ -\omega_2 & \omega_1 & 0 \end{pmatrix}.$$

Equations of motion (3)

- The equations of motion of the spacecraft are:

$$\begin{aligned}\ddot{\boldsymbol{R}} &= -\int_{MC_0} \frac{G\rho_0(M^\top \boldsymbol{Q})}{\|\boldsymbol{R}-\boldsymbol{Q}\|^3}(\boldsymbol{R}-\boldsymbol{Q})d\boldsymbol{Q} \\ &\overset{\boldsymbol{Q}=M\boldsymbol{s}}{=} -\int_{C_0} \frac{G\rho_0(\boldsymbol{s})}{\|M\boldsymbol{r}-M\boldsymbol{s}\|^3}(M\boldsymbol{r}-M\boldsymbol{s})d\boldsymbol{s} \\ &= M\left(-\int_{C_0} \frac{G\rho_0(\boldsymbol{s})}{\|\boldsymbol{r}-\boldsymbol{s}\|^3}(\boldsymbol{r}-\boldsymbol{s})d\boldsymbol{s}\right)\end{aligned}$$

- Since $\ddot{\boldsymbol{R}} = M(\ddot{\boldsymbol{r}} + 2\boldsymbol{\omega} \times \boldsymbol{r} + \boldsymbol{\omega} \times (\boldsymbol{\omega} \times \boldsymbol{r}))$, we have the equations in rotating coordinates,

$$\ddot{\boldsymbol{r}} + 2\boldsymbol{\omega} \times \dot{\boldsymbol{r}} = -\boldsymbol{\omega} \times (\boldsymbol{\omega} \times \boldsymbol{r}) + \nabla U(\boldsymbol{r}),$$

where

$$U(\boldsymbol{r}) = \int_{C_0} \frac{G\rho_0(\boldsymbol{s})}{\|\boldsymbol{r}-\boldsymbol{s}\|} d\boldsymbol{s}$$

is the **gravitational potential in body–fixed frame**.

Equations of motion (4)

- Taking coordinates $\boldsymbol{r} = (x, y, z)^\top$ s.t. the angular velocity vector is $\boldsymbol{\omega} = (0, 0, \omega)^\top$, the equations of motion are

$$\begin{cases} \ddot{x} - 2\omega\dot{y} &= \omega^2 x + \partial_x U \\ \ddot{y} + 2\omega\dot{x} &= \omega^2 y + \partial_y U \\ \ddot{z} &= \partial_z U \end{cases}$$

- In vector form again,

$$\ddot{\boldsymbol{r}} + 2\boldsymbol{\omega} \times \dot{\boldsymbol{r}} = \nabla_{\boldsymbol{r}} \left(\frac{\omega^2}{2}(x^2 + y^2) + U \right) =: \nabla_{\boldsymbol{r}} \Omega$$

- Dot–multiplying by $\dot{\boldsymbol{r}}$ at both sides and integrating: $\dot{r}^2/2 - \Omega$ is conserved.
- Taking momenta $\boldsymbol{p} = (p_x, p_y, p_z)$ defined by $\boldsymbol{p} = \dot{\boldsymbol{r}} + \boldsymbol{\omega} \times \boldsymbol{r}$, the equations of motion are Hamiltonian with Hamiltonian

$$H(\boldsymbol{r}, \boldsymbol{p}) = \frac{\dot{r}}{2} - \Omega = \frac{1}{2}(p_x^2 + p_y^2 + p_z^2) + \omega(yp_x - xp_y) - U(\boldsymbol{r}).$$

We'll refer to H as the **energy**.

Spherical harmonic expansion (1)

- The usual way to expand the potential is

$$
\begin{aligned}
U(\boldsymbol{r}) &= \int_{C_0} \frac{G\rho_0(\boldsymbol{s})}{\|\boldsymbol{r}-\boldsymbol{s}\|} d\boldsymbol{s} \\
&= \frac{\mu}{r} \sum_{m=0}^{\infty} \sum_{n=0}^{m} \left(\frac{R_{C_0}}{r}\right)^n P_{n,m}(\sin\phi) \Big(C_{n,m}\cos(m\lambda) + S_{n,m}\sin(m\lambda) \Big)
\end{aligned}
$$

where

$$
\begin{aligned}
(x,y,z) &= (r\cos\phi\cos\lambda, r\cos\phi\sin\lambda, r\sin\phi), \\
P_n(t) &= \frac{1}{2^n n!}\frac{d^n}{dt^n}(t^2-1)^n \qquad \text{(Legendre polynomial of deg } n\text{)}, \\
P_{n,m}(t) &= (1-t^2)^{m/2}\frac{d^m}{dt^m}P_n(t) \quad \text{(Legendre ass. fnc. of deg } n\text{, order } m\text{)},
\end{aligned}
$$

Spherical harmonic expansion (1)

- The usual way to expand the potential is

$$
\begin{aligned}
U(\boldsymbol{r}) &= \int_{C_0} \frac{G\rho_0(\boldsymbol{s})}{\|\boldsymbol{r}-\boldsymbol{s}\|} d\boldsymbol{s} \\
&= \frac{\mu}{r} \sum_{m=0}^{\infty} \sum_{n=0}^{m} \left(\frac{R_{C_0}}{r}\right)^n P_{n,m}(\sin\phi)\Big(C_{n,m}\cos(m\lambda) + S_{n,m}\sin(m\lambda)\Big)
\end{aligned}
$$

where

$$
\begin{aligned}
C_{n,m} &= \frac{2-\delta_{0,m}}{M_{C_0}} \frac{(n-m)!}{(n+m)!} \int_{C_0} \left(\frac{s}{R_{C_0}}\right)^n P_{n,m}(\sin\phi')\cos(m\lambda')\rho_0(\boldsymbol{s})d\boldsymbol{s}, \\
S_{n,m} &= \frac{2-\delta_{0,m}}{M_{C_0}} \frac{(n-m)!}{(n+m)!} \int_{C_0} \left(\frac{s}{R_{C_0}}\right)^n P_{n,m}(\sin\phi')\sin(m\lambda')\rho_0(\boldsymbol{s})d\boldsymbol{s}, \\
\boldsymbol{s} &= (r\cos\phi'\cos\lambda', r\cos\phi'\sin\lambda', r\sin\phi'),
\end{aligned}
$$

Spherical harmonic expansion (1)

- The usual way to expand the potential is

$$\begin{aligned} U(\boldsymbol{r}) &= \int_{C_0} \frac{G\rho_0(\boldsymbol{s})}{\|\boldsymbol{r}-\boldsymbol{s}\|} d\boldsymbol{s} \\ &= \frac{\mu}{r} \sum_{m=0}^{\infty} \sum_{n=0}^{m} \left(\frac{R_{C_0}}{r}\right)^n P_{n,m}(\sin\phi)\Big(C_{n,m}\cos(m\lambda) + S_{n,m}\sin(m\lambda)\Big) \end{aligned}$$

- The **solid spherical harmonic** of degree n, order m is

$$\frac{P_{n,m}(\sin\phi)}{r^{n+1}}(\cos(m\lambda) + i\sin(m\lambda))$$

Spherical harmonic expansion (2)

- It is usual to work with normalized coefficients:

$$\left\{ \begin{array}{c} \bar{C}_{n,m} \\ \bar{S}_{n,m} \end{array} \right\} = \sqrt{\frac{(n+m)!}{(2-\delta_{0,m})(2n+1)(n-m)!}} \left\{ \begin{array}{c} C_{n,m} \\ S_{n,m} \end{array} \right\},$$

$$\bar{P}_{n,m} = \sqrt{\frac{(2-\delta_{0,m})(2n+1)(n-m)!}{(n+m)!}} P_{n,m},$$

so that

$$U(\boldsymbol{r}) = \frac{\mu}{r} \sum_{m=0}^{\infty} \sum_{n=0}^{m} \left(\frac{R_{C_0}}{r} \right)^n \bar{P}_{n,m}(\sin\phi) \Big(\bar{C}_{n,m} \cos(m\lambda) + \bar{S}_{n,m} \sin(m\lambda) \Big).$$

- The coefficients $\bar{C}_{n,m}$, $\bar{S}_{n,m}$ are estimated by orbiting the body.
- For bodies never orbited (like Vesta), they are approximated by its definition from estimates of the shape of the body (C_0), its mass (M_{C_0}), and the composition of its interior, which gives an estimate of its density ρ_0. All these estimates are obtained from observations.

Evaluation of spherical harmonics

Cunningham, 1970

- The solid spherical harmonics

$$V_{n,m} := \frac{1}{r^{n+1}} P_{n,m}(\sin\phi)\Big(\cos(m\lambda) + i\sin(m\lambda)\Big),$$

can be computed through stable recurrences (Cunningham, 1970).

$$\begin{array}{ccccccc} V_{0,0} & & & & & & \\ \downarrow & \searrow & & & & & \\ V_{1,0} & & V_{1,1} & & & & \\ \downarrow & & \downarrow & \searrow & & & \\ V_{2,0} & & V_{2,1} & & V_{2,2} & & \\ \downarrow & & \downarrow & & \downarrow & \searrow & \\ \vdots & & \vdots & & \vdots & & \ddots \end{array}$$

Evaluation of spherical harmonics

Cunningham, 1970

- The solid spherical harmonics

$$V_{n,m} := \frac{1}{r^{n+1}} P_{n,m}(\sin\phi)\Big(\cos(m\lambda) + i\sin(m\lambda)\Big),$$

can be computed through stable recurrences (Cunningham, 1970).

- They cartesian derivatives are linear combinations of themselves:

$$\frac{\partial^{\alpha+\beta+\gamma} V_{n,m}}{\partial x^\alpha \partial y^\beta \partial z^\gamma} = i^\beta \sum_{j=0}^{\alpha+\beta} \frac{(-1)^{\alpha+\gamma-j}}{2^{\alpha+\beta}} \frac{(n-m+\gamma+2j)!}{(n-m)!} C_{\alpha,\beta,j} V_{l+\alpha+\beta+\gamma, m+\alpha+\beta-2j},$$

with

$$C_{\alpha,\beta,j} = \sum_{k=\max(0,j-\alpha)}^{\min(\beta,j)} (-1)^k \binom{\alpha}{j-k}\binom{\beta}{k}$$

$$V_{n,-m} = (-1)^m \frac{(n-m)!}{(n+m)!} V^*_{n,m}.$$

Vesta vs. the Earth

Coefficients of the expansion in spherical harmonics.

n	m	$C_{n,m}^{\text{Earth}}$	$S_{n,m}^{\text{Earth}}$	$C_{n,m}^{\text{Vesta}}$	$S_{n,m}^{\text{Vesta}}$
1	0	0	0	0	0
1	1	0	0	0	0
2	0	$-4.84 \cdot 10^{-6}$	0	$-4.08 \cdot 10^{-2}$	0
2	1	$-1.87 \cdot 10^{-10}$	$1.20 \cdot 10^{-9}$	$-3.25 \cdot 10^{-4}$	$1.50 \cdot 10^{-3}$
2	2	$2.44 \cdot 10^{-6}$	$-1.40 \cdot 10^{-6}$	$4.47 \cdot 10^{-3}$	$4.61 \cdot 10^{-3}$
3	0	$9.57 \cdot 10^{-7}$	0	$3.65 \cdot 10^{-3}$	0
3	1	$2.03 \cdot 10^{-6}$	$2.48 \cdot 10^{-7}$	$-1.12 \cdot 10^{-3}$	$-3.90 \cdot 10^{-4}$
3	2	$9.05 \cdot 10^{-7}$	$6.19 \cdot 10^{-7}$	$-1.16 \cdot 10^{-3}$	$-7.63 \cdot 10^{-4}$
3	3	$7.21 \cdot 10^{-7}$	$1.41 \cdot 10^{-6}$	$-6.72 \cdot 10^{-4}$	$5.48 \cdot 10^{-4}$

Vesta gravity environment


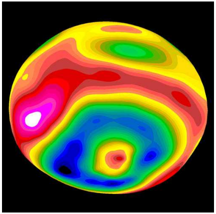


Parameter	4 Vesta	units
Gravitational parameter	17.8	km^3/s^2
Rotational period	5.342	*hrs*
Spherical Harmonic Gravity Coefficients	8x8	(HST estimated)

Outline

1. Model setting
2. Resonant dynamics
3. Ballistic resonance crossing
4. Polar families of p.o.
5. Conclusions

Equilibria

- true 1:1 resonant orbits with a 1–point ground–track ("geostationary") are seen as equilibria in the rotating frame.
- There are 4 equilibria in the geostationary belt (e.g. Kaula 1966).
- There are 4 equilibria in a 2×2 grav. model for Vesta (Scheeres 1994).
- In a full 8×8 model for Vesta, still 4 points are found.

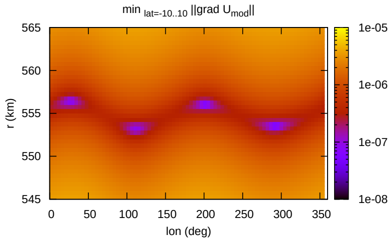

Point	x	y	z	Stability	Jacobi Energy (km^2/s^2)
P_1	499.9795	247.0219	-1.4636	unstable	9.7865×10^{-2}
P_2	-202.9481	515.9822	0.1698	stable	9.7489×10^{-2}
P_3	-521.6020	-196.3435	-1.0015	unstable	9.7833×10^{-2}
P_4	198.8385	-517.9082	-1.3808	stable	9.7515×10^{-2}

Equilibria

- true 1:1 resonant orbits with a 1–point ground–track ("geostationary") are seen as equilibria in the rotating frame.
- There are 4 equilibria in the geostationary belt (e.g. Kaula 1966).
- There are 4 equilibria in a 2×2 grav. model for Vesta (Scheeres 1994).
- In a full 8×8 model for Vesta, still 4 points are found.

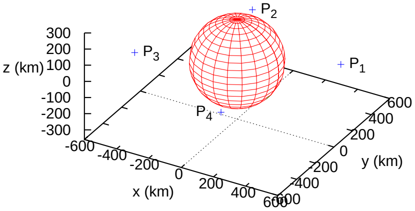

Point	x	y	z	Stability	Jacobi Energy (km^2/s^2)
P_1	499.9795	247.0219	-1.4636	unstable	9.7865×10^{-2}
P_2	-202.9481	515.9822	0.1698	stable	9.7489×10^{-2}
P_3	-521.6020	-196.3435	-1.0015	unstable	9.7833×10^{-2}
P_4	198.8385	-517.9082	-1.3808	stable	9.7515×10^{-2}

Eigenvalues of equilibria

- Eigenvalues of equilibria:

$$\begin{array}{llllll} j & = & 1,3, & \text{Spec}\, D\vec{\mathbf{F}}(P_j) & = & \{\pm\lambda^j, \pm i\omega_p^j, \pm i\omega_v^j\}, & \text{(saddle} \times \text{center} \times \text{center case)} \\ k & = & 2,4, & \text{Spec}\, D\vec{\mathbf{F}}(P_k) & = & \{\pm i\omega_1^k, \pm i\omega_2^k, \pm i\omega_3^k\}, & \text{(center} \times \text{center} \times \text{center case)} \end{array}$$

  The eigenvectors of eigenvalues $\pm i\omega_p^j$ are close to planar.
  The eigenvectors of eigenvalues $\pm i\omega_v^j$ are close to vertical.

- Numerical values:

j	λ^j	ω_p^j	ω_v^j
1	6.27114×10^{-5}	3.21174×10^{-4}	3.38038×10^{-4}
3	5.91673×10^{-5}	3.21221×10^{-4}	3.37354×10^{-4}

- $\lambda^1, \lambda^3 \approx 6 \times 10^{-5} \Longrightarrow$ the distance to the fixed point is multiplied or divided by $e \approx 2.7$ each $1/\lambda^j \approx 0.17 \times 10^5\,\text{s} = 4.6\,\text{h}$ (by 100 every 21 h).
- Lyapunov's center theorem ensures the generation of planar and vertical families.
- Their limit periods (close to the fixed point) are (Vesta's rotation period: 5.342 h)

j	$2\pi/\omega_p^j$	$2\pi/\omega_v^j$
1	5.43 h	5.16 h
3	5.43 h	5.17 h

Zero-velocity surfaces

Since

$$C := J(\vec{r}, \dot{\vec{r}}) = 2U + \omega^2(x^2 + y^2) - (\dot{x}^2 + \dot{y}^2 + \dot{z}^2)$$

is a constant of motion, and

$$\dot{x}^2 + \dot{y}^2 + \dot{z}^2 = J(\vec{r}, \vec{\mathbf{0}}) - C,$$

motion is only permitted if $J(\vec{r}, \vec{\mathbf{0}}) - C \geq 0$.

Contours of $J(\vec{r}, \vec{\mathbf{0}})$:

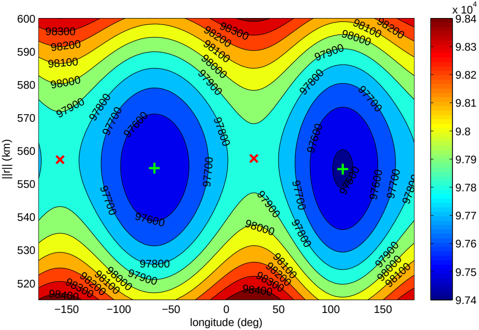

Zero-velocity surfaces

Since

$$C := J(\vec{r}, \dot{\vec{r}}) = 2U + \omega^2(x^2 + y^2) - (\dot{x}^2 + \dot{y}^2 + \dot{z}^2)$$

is a constant of motion, and

$$\dot{x}^2 + \dot{y}^2 + \dot{z}^2 = J(\vec{r}, \vec{\mathbf{0}}) - C,$$

motion is only permitted if $J(\vec{r}, \vec{\mathbf{0}}) - C \geq 0$.

Contours of $J(\vec{r}, \vec{\mathbf{0}})$.

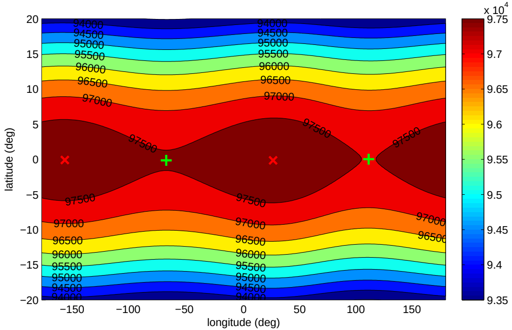

Lyapunov families of p.o.

They are the non-linear versions of the linear, central oscillations around P_1, P_3.

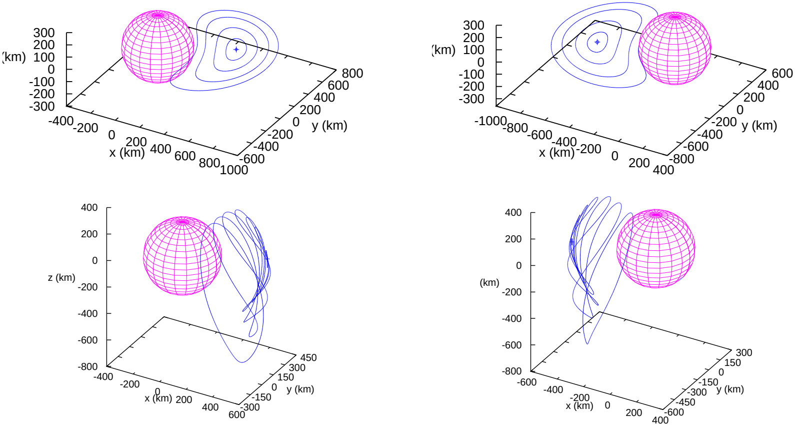

Lyapunov families of p.o.

They are the non-linear versions of the linear, central oscillations around P_1, P_3.

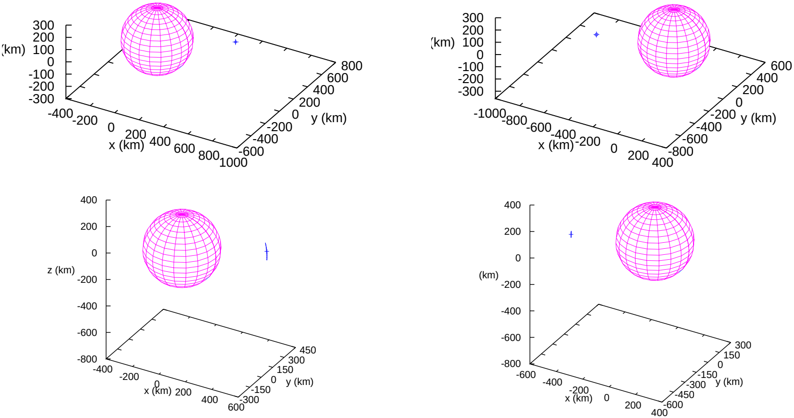

Lyapunov families of p.o.

They are the non-linear versions of the linear, central oscillations around P_1, P_3.

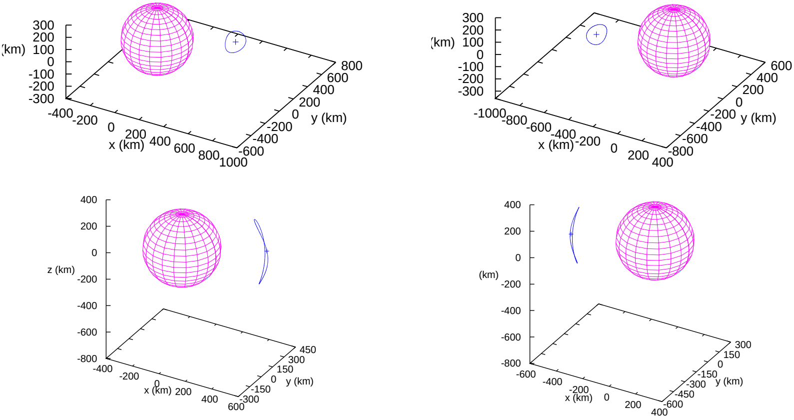

Lyapunov families of p.o.

They are the non-linear versions of the linear, central oscillations around P_1, P_3.

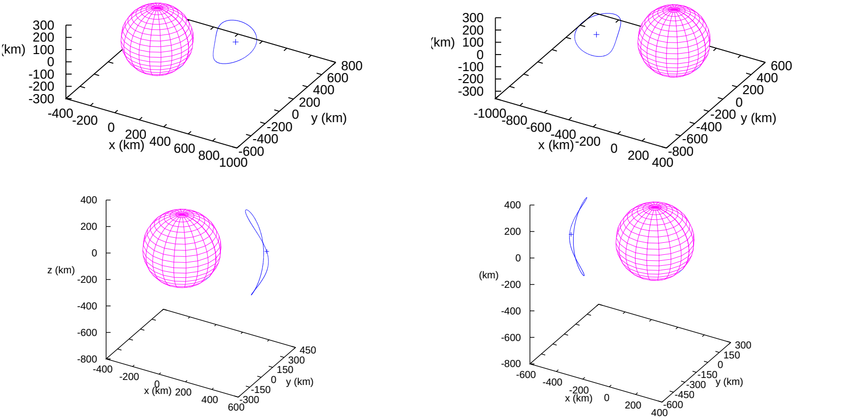

Lyapunov families of p.o.

They are the non-linear versions of the linear, central oscillations around P_1, P_3.

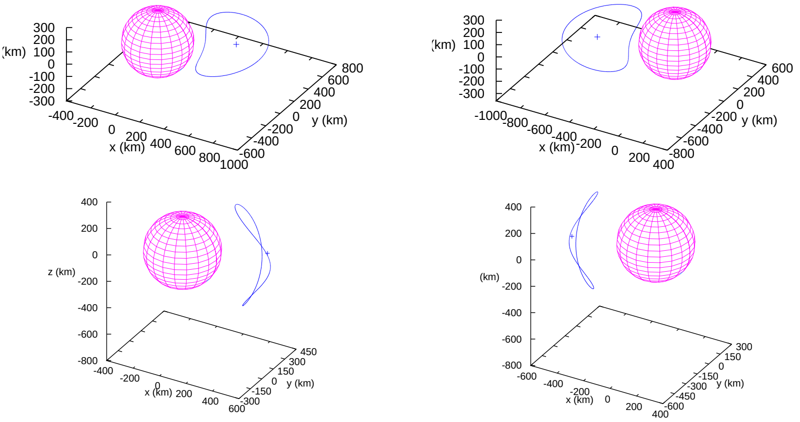

They are the non-linear versions of the linear, central oscillations around P_1, P_3.

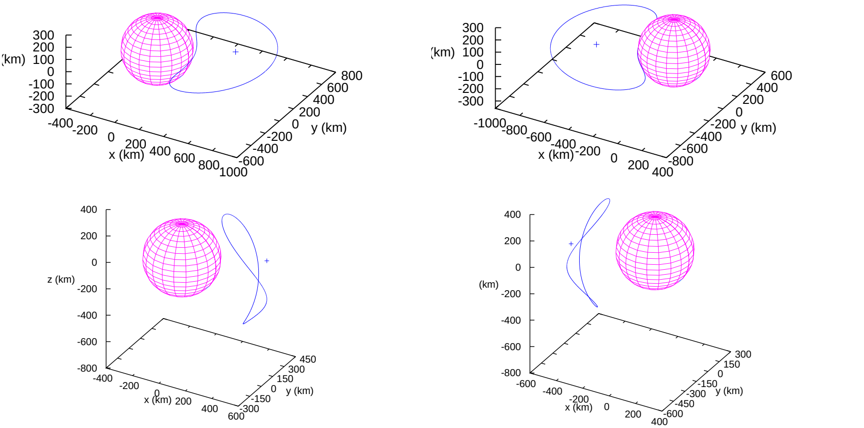

Lyapunov families of p.o.

They are the non-linear versions of the linear, central oscillations around P_1, P_3.

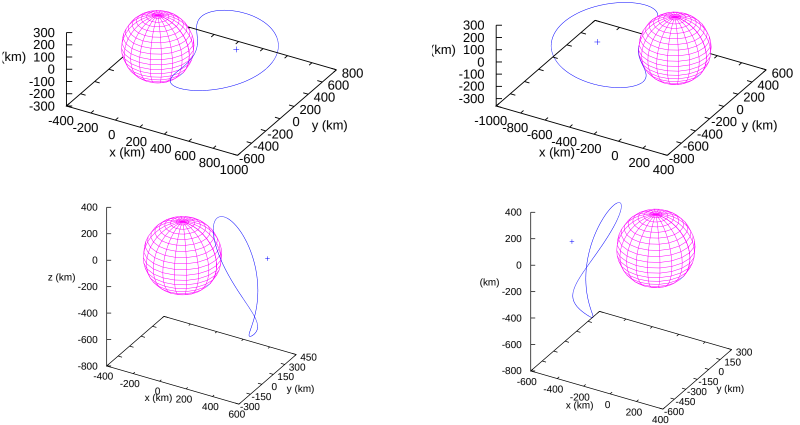

Lyapunov families of p.o.

They are the non-linear versions of the linear, central oscillations around P_1, P_3.

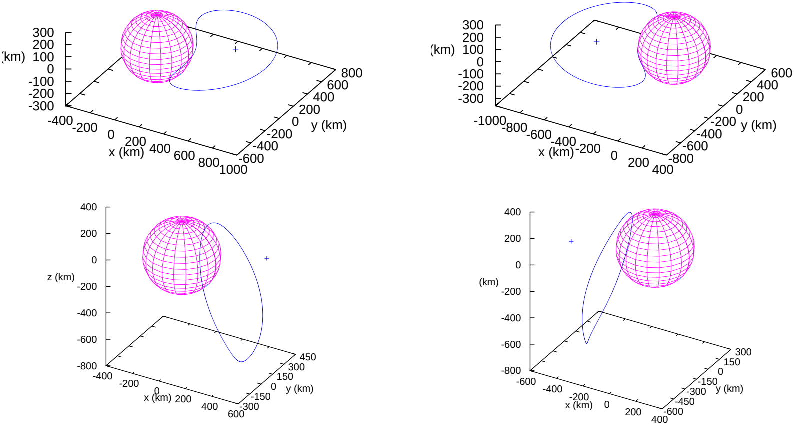

Lyapunov families of p.o.

They are the non-linear versions of the linear, central oscillations around P_1, P_3.

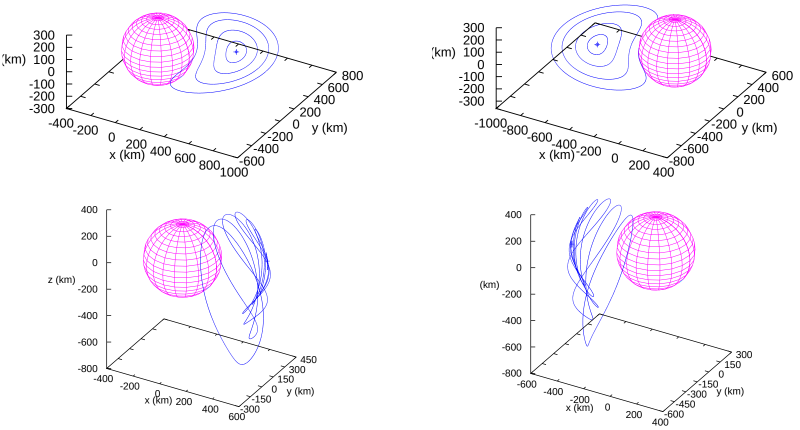

Lyapunov families of p.o.

Characteristic curves:

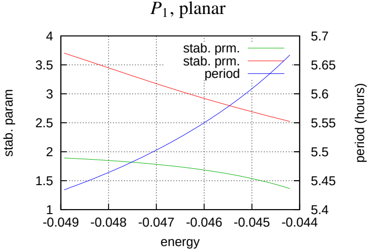

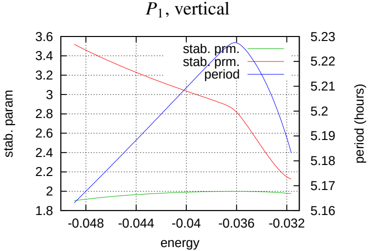

Sizes:

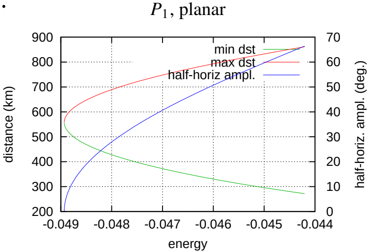

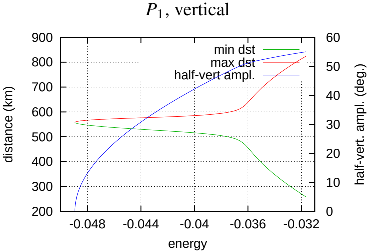

Geostationary–belt–like behavior

- Reproduced by the invariant manifolds of the Lyapunov p.o.
- To a larger scale, due to their size.

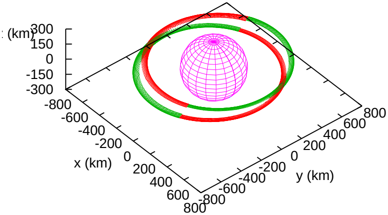

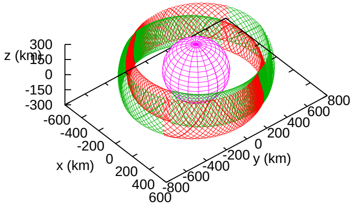

Manifolds of p.o. providing transfers

The suitable branches need to be chosen.

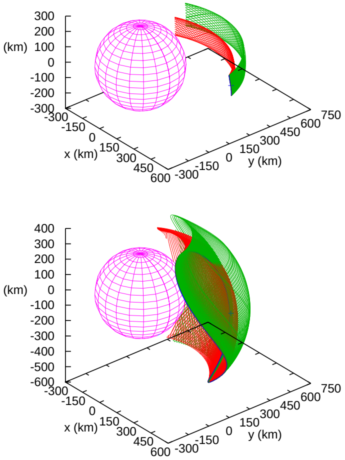

The suitable branches need to be chosen.

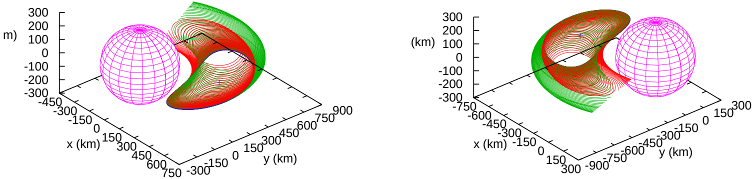

Minimum–maximum distance to Vesta of manifold tubes

From sections of vertical planes of the longitude of the P_1, P_3 fixed point plus 90 degrees.
Note that $a_{1:1 \text{ res}} = 550.416$ km.

Planar fam., P_1

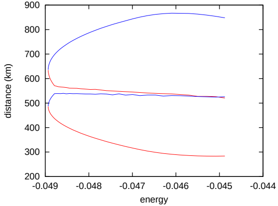

Vertical fam., P_1

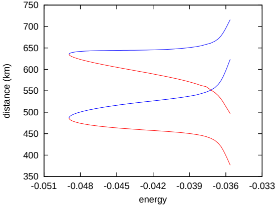

Planar fam., P_3

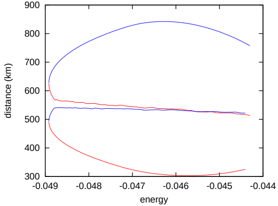

Vertical fam., P_3

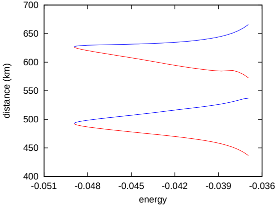

Outline

1. Model setting
2. Resonant dynamics
3. Ballistic resonance crossing
4. Polar families of p.o.
5. Conclusions

- Geometry in the Planar Circular Restricted Three–Body Problem.

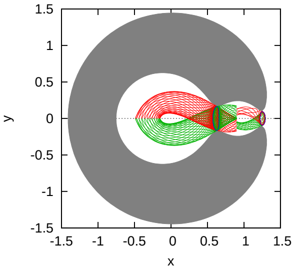

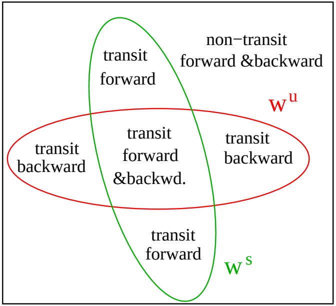

Poincare section (qualitative)

- In 3D, all the tori of an energy level would need to be considered.

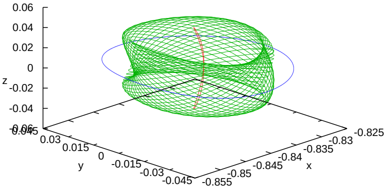

Transit orbits

- Geometry in the Planar Circular Restricted Three–Body Problem.

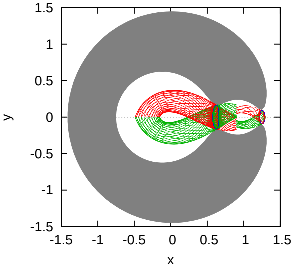

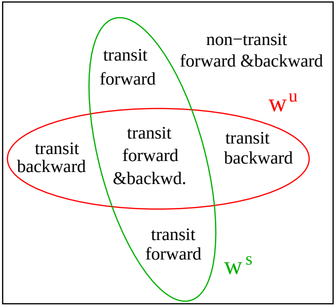

Poincare section (qualitative)

- Generate transit orbits shooting close to the p.o.

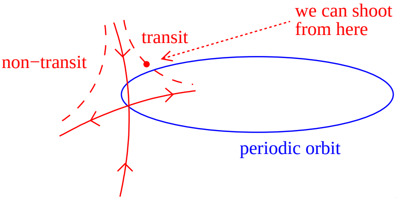

Generating ballistic transfers

- Eigenvalues of the monodromy matrix:

$$\operatorname{Spec} D\vec{\phi}_T(\vec{\mathbf{X}}_0) = \{1, 1, \Lambda^u, \Lambda^s, e^{i\nu}, e^{-i\nu}\}$$

  for $\Lambda^u = \Lambda > 1$, $\Lambda^s = 1/\Lambda$, $\nu > 0$.
- $\vec{\mathbf{V}}^u, \vec{\mathbf{V}}^s$ eigenvectors corresponding to Λ^u, Λ^s.
- Parametrization of the linear approximation of the stable–unstable manifold of the p.o.:

$$\begin{aligned}\vec{\psi}(\theta, \xi^u, \xi^s) &= \vec{\phi}_{\frac{\theta}{2\pi}T}(\vec{\mathbf{X}}_0) \\ &\quad + \left((\Lambda^u)^{-\theta/(2\pi)} D\vec{\phi}_{\frac{\theta}{2\pi}T}(\vec{\mathbf{X}}_0)\vec{\mathbf{V}}^u\right)\xi^u \\ &\quad + \left((\Lambda^s)^{-\theta/(2\pi)} D\vec{\phi}_{\frac{\theta}{2\pi}T}(\vec{\mathbf{X}}_0)\vec{\mathbf{V}}^s\right)\xi^s\end{aligned}$$

Generating ballistic transfers

- Parametrization of the linear approximation of the stable–unstable manifold of the p.o.:

$$
\begin{aligned}
\vec{\psi}(\theta,\xi^u,\xi^s) \quad = \quad & \vec{\phi}_{\frac{\theta}{2\pi}T}(\vec{\mathbf{X}}_0) \\
& +\left((\Lambda^u)^{-\theta/(2\pi)} D\vec{\phi}_{\frac{\theta}{2\pi}T}(\vec{\mathbf{X}}_0)\vec{\mathbf{V}}^u\right)\xi^u \\
& +\left((\Lambda^s)^{-\theta/(2\pi)} D\vec{\phi}_{\frac{\theta}{2\pi}T}(\vec{\mathbf{X}}_0)\vec{\mathbf{V}}^s\right)\xi^s
\end{aligned}
$$

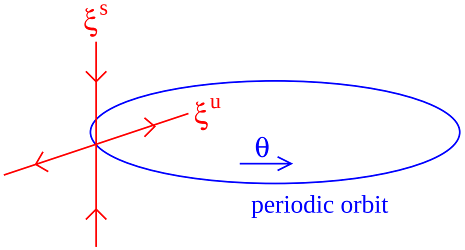

Generating ballistic transfers

We have integrated forward and backward in time from $\vec{\psi}(\theta, \xi, \xi)$ for

$$\begin{aligned} \theta &= j(2\pi/50), \quad 0 \le j \le 49 \\ \xi &= 0.1,\ 1,\ 10\,\mathrm{km} \end{aligned}$$

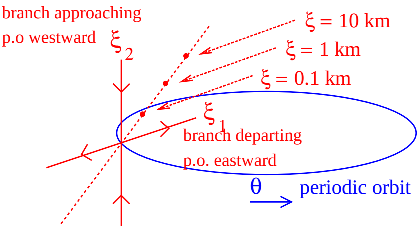

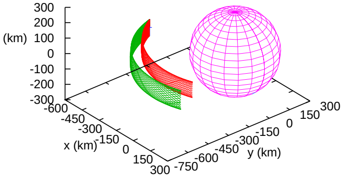

Ballistic transfers TOF and distance

Left y axis: TOF for $\xi = 0.1\,\mathrm{km}$, $\xi = 1\,\mathrm{km}$, $\xi = 10\,\mathrm{km}$.
Right y axis: difference between maximum and minimum distance to Vesta along the transfer.

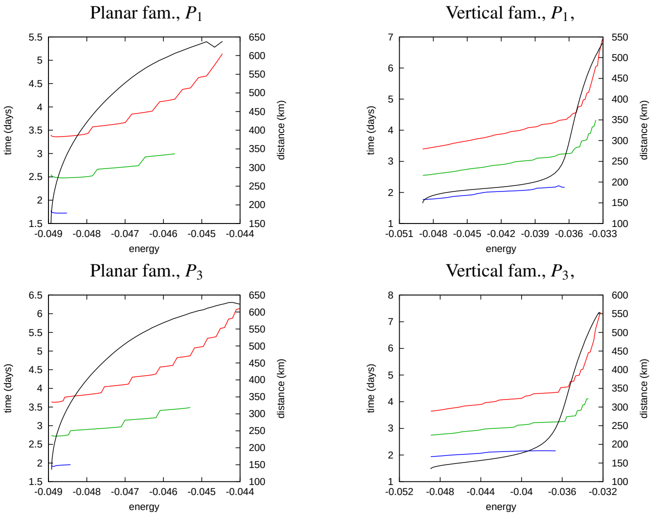

Some sample transfers

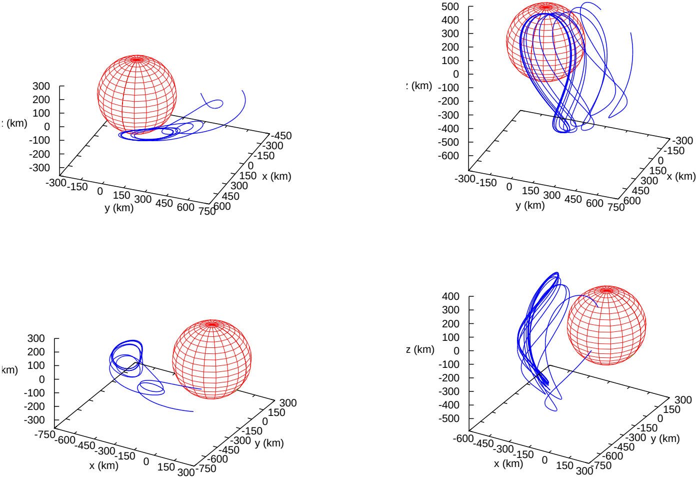

Outline

1. Model setting
2. Resonant dynamics
3. Ballistic resonance crossing
4. Polar families of p.o.
5. Conclusions

Polar families of p.o.

Around P_1 (left column) and P_3 (right column).

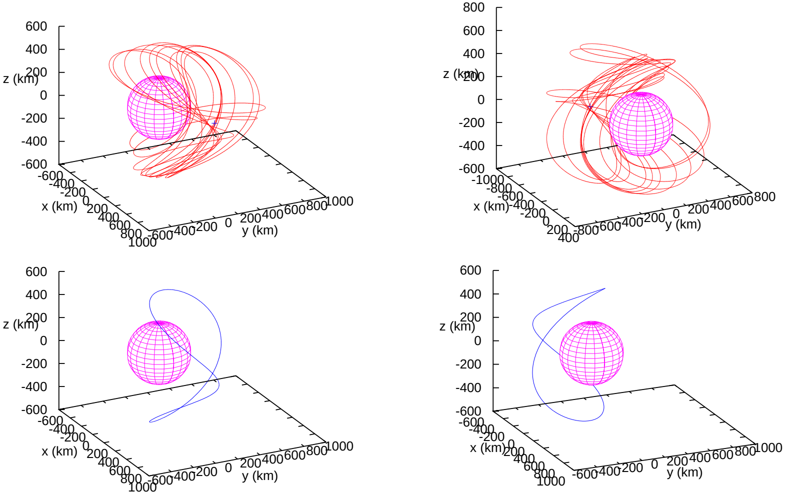

Polar families of p.o.

Around P_1 (left column) and P_3 (right column).

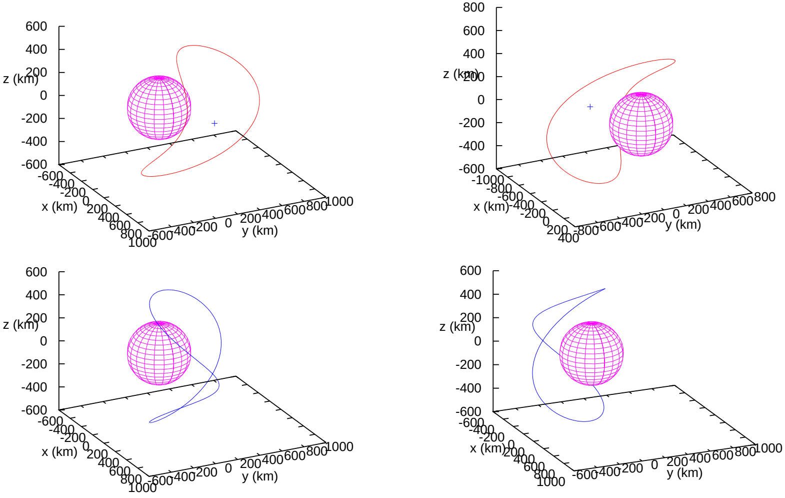

Polar families of p.o.

Around P_1 (left column) and P_3 (right column).

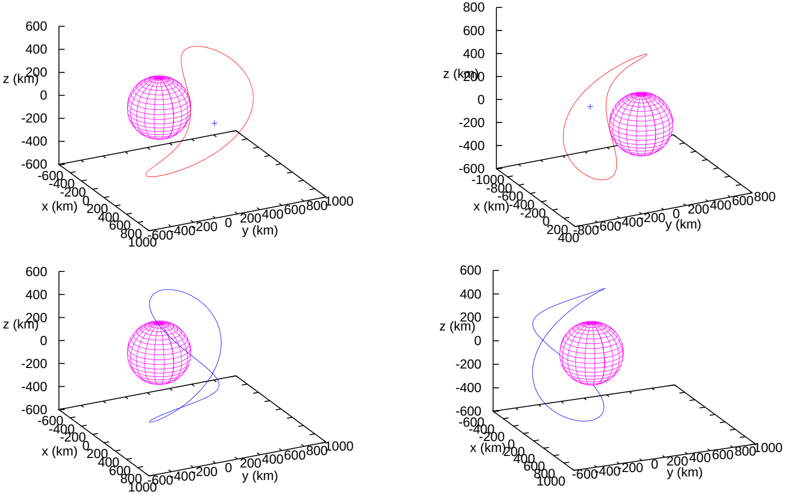

Polar families of p.o.

Around P_1 (left column) and P_3 (right column).

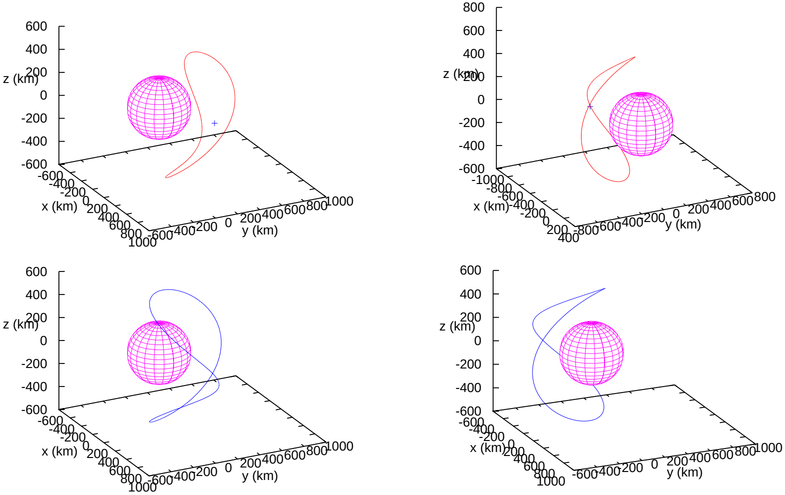

Polar families of p.o.

Around P_1 (left column) and P_3 (right column).

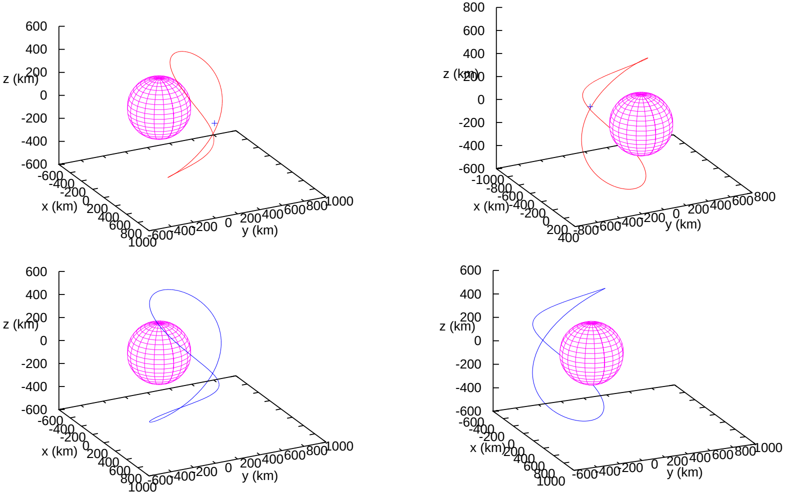

Around P_1 (left column) and P_3 (right column).

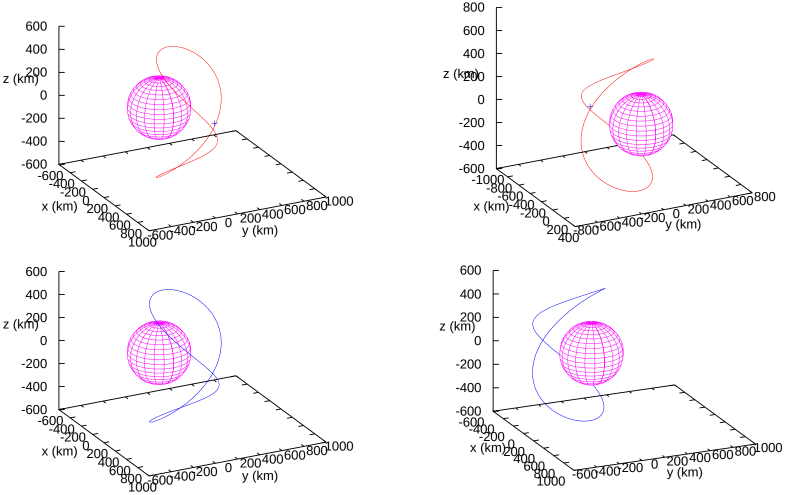

Polar families of p.o.

Around P_1 (left column) and P_3 (right column).

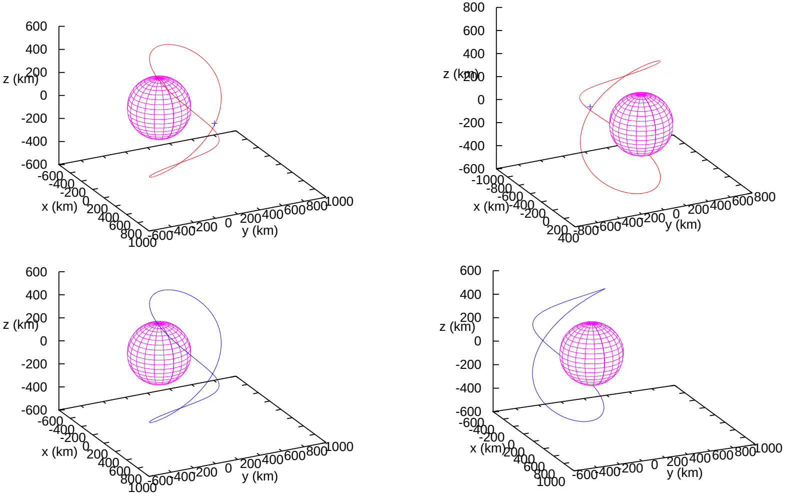

Polar families of p.o.

Around P_1 (left column) and P_3 (right column).

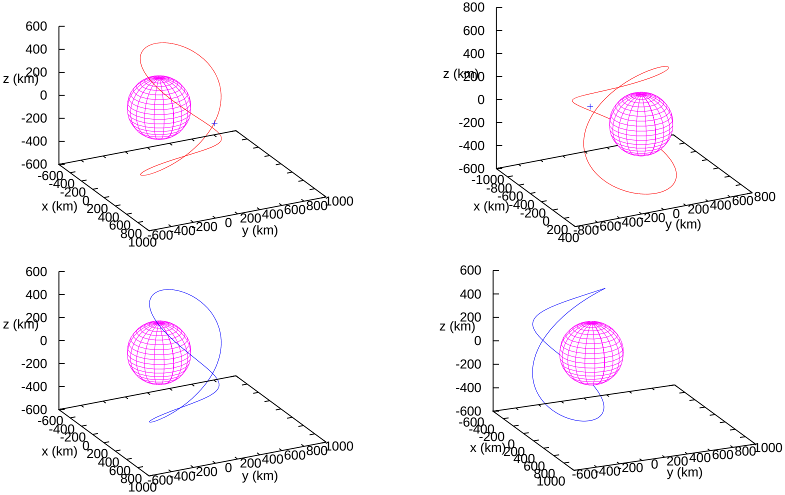

Polar families of p.o.

Around P_1 (left column) and P_3 (right column).

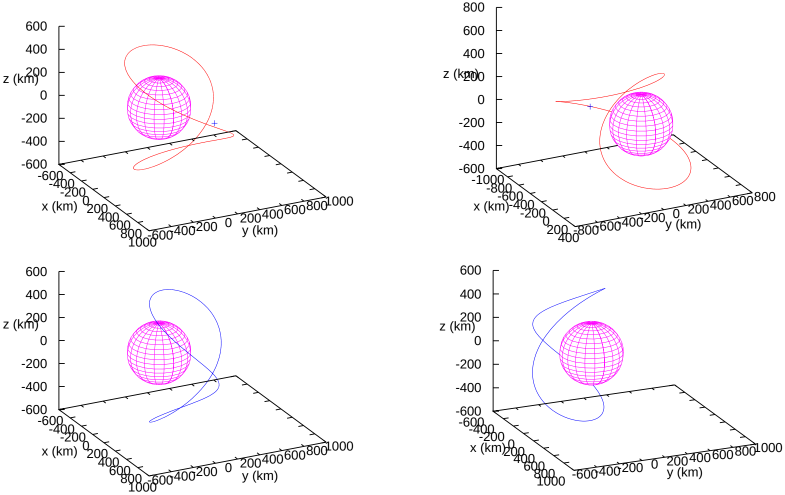

Polar families of p.o.

Around P_1 (left column) and P_3 (right column).

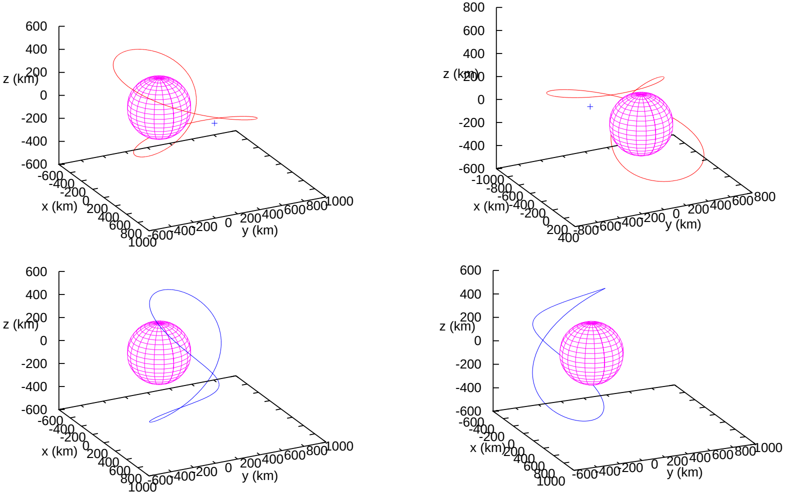

Polar families of p.o.

Around P_1 (left column) and P_3 (right column).

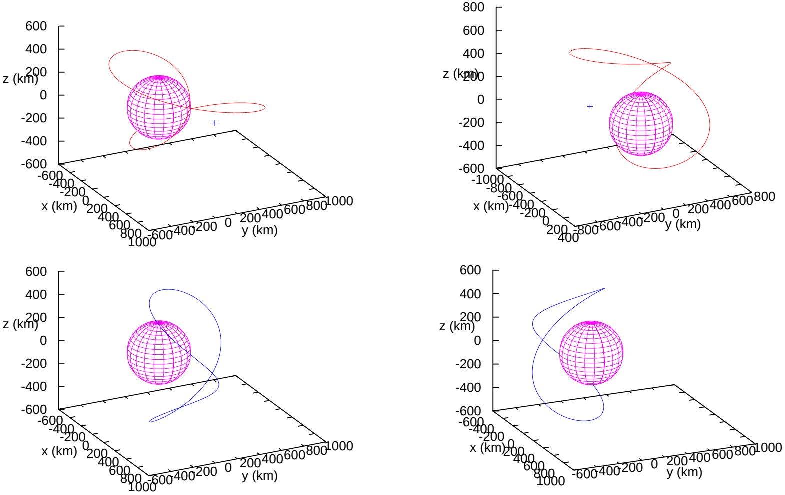

Polar families of p.o.

Around P_1 (left column) and P_3 (right column).

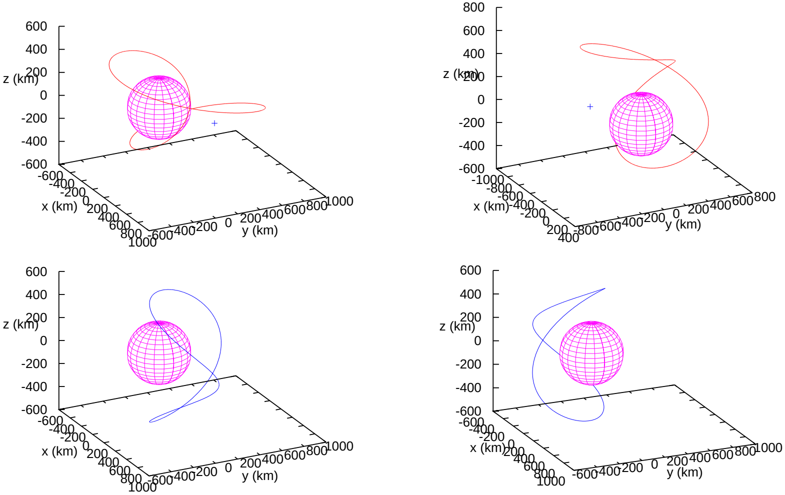

Stability parameters

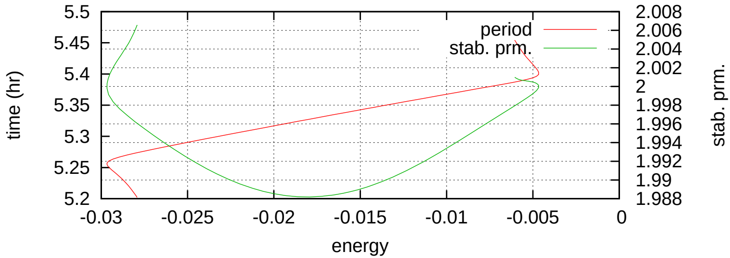

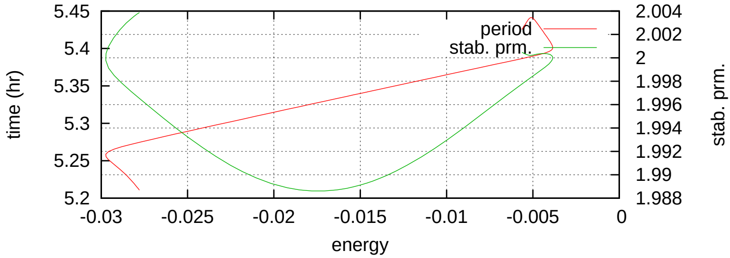

Outline

1. Model setting
2. Resonant dynamics
3. Ballistic resonance crossing
4. Polar families of p.o.
5. Conclusions

Conclusions & Outlook

- Dynamics near the 1:1 exhibits similar behavior to motion near collinear LP, and also to the Earth's geostationary belt, but different length and time scales.
- Dynamics seems to be **robust** with respect to gravity field uncertainties (same number and type of equilibria as in simplified models).
- Significant orbit altitude changes (about 300 km) can be done through invariant manifolds of Lyapunov p.o.
  They can be done both through near–equatorial orbits and inclined ones.
- We have presented a **systematic** method of computing these orbit transfers, and characterized a selected set of such solutions.

Future work:

- Characterization of the whole set of such transfers.
- More complete sensitivity analysis with respect to gravity field uncertainties.
- Check for existence of homoclinic connections "closing" the geostationary belt.

& Thank You!

Acknowledgements

- The authors would like to thank Greg Whiffen of the Dawn navigation team at JPL.
- J.M.M. is partially supported by the Spanish & Catalan grants MCyT/FEDER MTM2008–01486, MCyT/FEDER MTM2006-05849/Consolider, and 2009SGR410.
- Part of this work as been performed at the Jet Propulsion Laboratory, California Institute of Technology, which is under contract with the National Administration for Space and Aeronautics.